Journal of Renewable Materials

Tech Science Press

DOI: 10.32604/jrm.2021.015066

ARTICLE

Soy Protein Isolate Non-Isocyanates Polyurethanes (NIPU) Wood Adhesives

Xinyi Chen[1,2], Antonio Pizzi[1,*], Xuedong Xi[1,2], Xiaojian Zhou[2], Emmanuel Fredon[1] and Christine Gerardin[3]

[1]LERMAB, University of Lorraine, Epinal, 88000, France

[2]Yunnan Key Laboratory of Wood Adhesives and Glue Products, Southwest Forestry University, Kunming, 650224, China

[3]LERMAB, University of Lorraine, Nancy, 54000, France

[*]Corresponding Author: Antonio Pizzi. Email: antonio.pizzi@univ-lorraine.fr

Received: 19 November 2020 Accepted: 11 December 2020

ABSTRACT

Soy-protein isolate (SPI) was used to prepare non-isocyanate polyurethane (NIPU) thermosetting adhesives for wood panels by reacting it with dimethyl carbonate (DMC) and hexamethylene diamine. Both linear as well as branched oligomers were obtained and identified, indicating how such oligomer structures could further cross-link to form a hardened network. Unusual structures were observed, namely carbamic acid-derived urethane linkages coupled with lactam structures. The curing of the adhesive was followed by thermomechanical analysis (TMA). It appeared to follow a two stages process: First, at a lower temperature (maximum 130°C), the growth of linear oligomers occurred, finally forming a physically entangled network. This appeared to collapse and disentangle, causing a decrease of MOE, as the temperature increases. This appears to be due to the ever more marked Brownian movements of the linear oligomer chains with the increase of the temperature. Second, chemical cross-linking of the chains appeared to ensue, forming a hardened network. This was shown by the thermomechanical analysis (TMA) showing two distinct MOE maxima peaks, one around 130°C and the other around 220°C, with a very marked MOE decrease between the two. Plywood panels were prepared and bonded with the SPI-NIPU wood adhesive and the results obtained are presented. The adhesive appeared to pass comfortably the requirements for dry strength of relevant standards, showing to be suitable for interior grade plywood panels. It did not pass the requirements for wet tests. However, addition of 15% of glycerol diglycidyl ether improved the wet tests results but still not enough to satisfy the standards requirements.

KEYWORDS

Bio-based wood adhesives; soy protein isolate; non-isocyanate polyurethanes (NIPU); wood panels; MALDI ToF

1 Introduction

Soy protein has been and is one of the protein of choice to formulate wood adhesives. This is so as it is a renewable raw material of vegetable origin, widely available, and relatively inexpensive [1]. It can be applied (i) In several forms as an additive to traditional synthetic wood adhesives, or (ii) Used as a wood adhesive after partial hydrolysis and modifications [2]. Nonetheless, this adhesive material presents a few drawbacks, such as an insufficient water resistance, its improvement being one of the subjects of present research. The approach most generally used to improve this aspect is by adding a chemical cross-linker to soy protein

isolate [3–9]. More recently good results have been obtained by reinforcing soy adhesives with condensed tannins [10–12] as well by preparing wood adhesives from soy flour by generating higher molecular weight, non-volatile non-toxic aldehydes by periodate specific oxidation [13,14].

Polyurethanes are a ubiquitous and widely used material for a number of applications, such as coatings, varnishes, foams and wood adhesives in structural glulam and finger-jointing. Polyurethanes are to-day prepared using polymeric isocyanate. However, isocyanates are classed as toxic. Polymeric diphenylmethane diisocyanate (p-MDI) is used for wood adhesives. p-MDI is also used as a modifier/crosslinker to improve the performance of protein adhesives [15,16]. The toxicity of p-MDI has focused research on its substitution by preparing polyurethanes without isocyanates (NIPU). Several approaches are used for this, namely by reacting hydroxyl groups-carrying materials with one or two cycles organic carbonates or CO_2 and diamines [17–21]. This research has mainly been directed to the preparation of foams and coatings [22–26]. All these are using oil-derived synthetic-based materials to prepare NIPUs. More recently, successful attempts to produce NIPUs from natural materials rich in hydroxyl groups have been reported [27–37]. These have the additional characteristic to have simplified the procedure by using a cheaper aliphatic carbonate by eliminating the reaction of preparing cyclic carbonates [27–37]. Among these, glucose-and sucrose-based NIPUs prepared with dimethyl carbonate and hexamethylene diamine were used to bond wood joint and particleboard with encouraging results [34,35]. Thus, soy-based non-isocyanate polyurethanes are an interesting route to pursue, considering the amount of hydroxyl groups and amino groups of which SPI's aminoacids are rich, and also considering the possibility of reaction of the numerous amide group of the peptide grouping in the constitutive skeletal chain of proteins. The work described here is then aimed at preparing a NIPU wood adhesive based on soy protein isolate presenting good bonding characteristics.

2 Experimental

2.1 Materials

Soy protein isolate was supplied by Ruikang Biotechnology Co., Ltd. (Dezhou, China). Commercial glycerol diglycidyl ether (GDE, technical grade), hexamethylene diamine 98%, and dimethyl carbonate were bought from Sigma-Aldrich (Saint Louis, France).

2.2 Preparation of SPI-NIPU Adhesive

The SPI-NIPU adhesive was prepared as follows: 80 g SPI is dissolved in 400 g of deionized water under magnetic stirring, then 54 g dimethyl carbonate is added and the mixture heated to 60°C for 120 min. Then 105 g hexamethylenediamine are then added and heated to 90°C for another 2 h, then cooled to room temperature. The mixture can be roto-evaporated under reduced pressure at 55°C to eliminate the excess of water and to obtain a final resin solids content of 45%. with a viscosity of 26.9 ± 1 Pa•s.

2.3 Thermomechanical Analysis (TMA)

The resins were tested by thermomechanical analysis. The samples were prepared by applying each adhesive between two beech wood plies, with dimensions of 21 mm × 6 mm × 1.1 mm. These beech-resin-beech sandwiches were tested in non-isothermal mode between 25°C and 250°C at a heating rate of 10 °C/minute with a Mettler Toledo 40 TMA equipment (Mettler Toledo, Zurich, Switzerland). They were tested in three-point bending on a span of 18 mm exercising a force cycle of 0.1/0.5 N on the specimens, with each force cycle of 12 seconds (6 s/6 s). The classical mechanics relationship between force and deflection

$$E = [L3/(4bh3)][F/(f_{wood} - f_{adhesive})]$$

where L = the length of the sample; b = its width; h = its thickness; F = the force applied f_{wood} the deflection of the wood and $f_{adhesive}$ the deflection of the wood adhesive sandwich under test. This equation allows the calculation of the Young's modulus E for each case tested. Such a measuring system has been introduced and is used to follow the progressive hardening of the adhesive with the increase of temperature and to indicate comparatively if an adhesive system is faster or slower hardening and if it gives stronger joints than another one.

2.4 ATR-FT-MIR Analysis

All of the samples were analyzed with a PerkinElmer Frontier ATR-FT-MIR provided by an ATR Miracle diamond crystal. The powder and liquid samples were laid on the diamond eye (1.8 mm) of the ATR equipment and the contact for the sample was ensured by tightly screwing the clamp device. Each extract was scanned registering the spectrum with 32 scans with a resolution of 4 cm^{-1} in the wave number range between 600 and 4000 cm^{-1}.

2.5 MALDI-ToF Analysis

Samples for matrix assisted laser desorption ionization time-of-flight (MALDI-ToF) analysis were prepared by first dissolving 7.5 mg of sample powder in 1mL of a 50:50 v/v acetone/water solution. Then 10 mg of this solution was added to 10 µL of a 2,5-dihydroxy benzoic acid (DHB) matrix. The locations dedicated to the samples on the analysis plaque were first covered with 2 µL of a NaCl solution 0.1 M in 2:1 v/v methanol/water, and predried. Then 1.5 µL of the sample solution was placed on its dedicated location and the plaque was dried again. Red phosphorous was to standardize the MALDI equipment. MALDI-ToF spectra were obtained using an Axima-Performance mass spectrometer from Shimadzu Biotech (Kratos Analytical Shimadzu Europe Ltd., Manchester, UK) using a linear polarity-positive tuning mode. The measurements were carried out making 1000 profiles.

2.6 Three-Layer Plywood Preparation and Testing

The performance of the SPI-NIPU adhesive was tested by preparing laboratory plywood panels and evaluating their shear strength dry, after 24 hours cold water soaking, and after 3 h in water at 63°C. The plywood panels of 400 mm × 200 mm × 5 mm were prepared for each adhesive using 2 mm poplar (*Populus tremuloides*) veneers. The glue spread used was of 300 g/m^2 double glue line, and hot-pressing time was of 6 minutes at 1.25 MPa pressure at a temperature of 200°C based on the consequence of the TMA trace. After hot pressing the plywood was stored under ambient conditions (20°C and 12% relative humidity) for 48 hours then it was cured and tested the dry shear strength, 24 h cold water soaking strength and for strength after 3 h at 63°C in water according to China National Standard GB/T 14074 (2006) [38], China National Standard GB/T17657 (1999) [39], and European Norm EN 636:2012 (2012) [40]. To reinforce the SPI-NIPU plywood also panels to which 10% or 15% by weight of a biosourced glycerol diglycidyl ether (GDE) were added to the SPI-NIPU based on solids were also pressed and tested under the same conditions.

3 Results and Discussion

3.1 MALDI ToF Analysis

The MALDI ToF analysis shows that SPI-NIPU urethane linkages do form with at least some of the soy protein amino acids. However, the analysis also shows that for SPI it is not a straightforward reaction to NIPUs as described for other bio-sourced materials (Figs. 1a–1d). The assignments for the relevant peaks of the spectra are shown in Tab. 1. Thus, the peaks in Fig. 1a at 189 Da and 215 Da can be assigned to the reaction product of leucine with DMC without and with Na^+ being present, respectively, hence to a structure of Type (I):

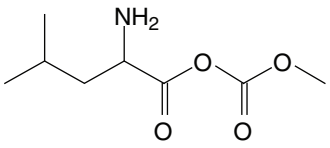

I

The same structure is present for 284 Da and 311 Da which can be assigned to triptofan-DMC without or with Na^+. At 271 Da the structure can be attributed to serine-DMC-hexamethylene diamine $+Na^+$. However, at 271 Da and 295 Da the structure that can be deduced is leucine-DMC-hexamethylene diamine without or with Na^+ of Structure (II)

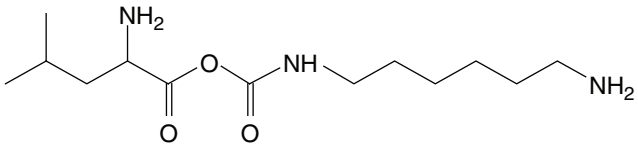

II

It must be clearly pointed out that while a urethane linkage, namely R-NH-COO-R is formed, the structure so formed is also a lactam, as indicated by the -CO-O-CO- structure. The same type of urethane/lactam linkage is found also at 339 Da and 368 Da these being respectively arginine-DMC-diamine + Na^+ and tryptophan-DMC-diamine + Na^+. The small peak at 453 Da indicates the formation of a different oligomer, namely: leucine-DMC-diamine-DMC-leucine $+Na^+$, hence a more complex structure of Type (III):

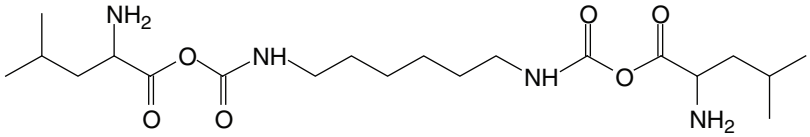

III

The same type of structure but involving different amino acids is present at 495 Da, 539 Da and 602 Da, these oligomers being respectively leucine-DMC-amine-DMC-arginine + Na^+, arginine-DMC-amine-DMC-arginine + Na^+ and tryptophan-DMC-amine-DMC-tryptophan + Na^+.

It must be pointed out that:

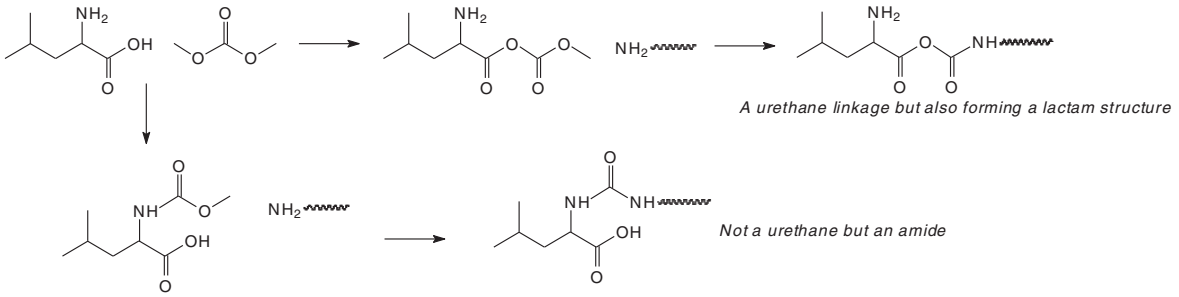

The first one of these reactions can be schematically summarized as

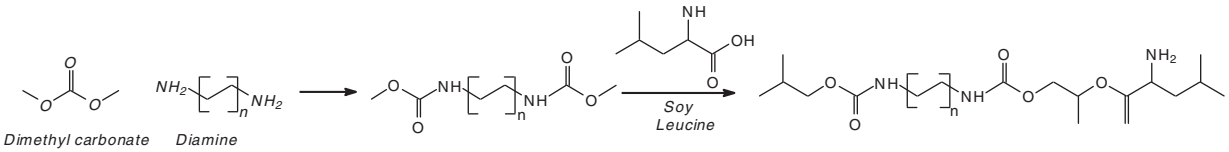

This reaction, as seen, leads to urethanes that eventually share a lactam structure. To avoid the presence of urethane/lactam type structure then a longer carbonate, cyclic or not should be used.

2. That after urethane dimers are formed such as those of the peaks at 453 Da, 495 Da, 539 Da and 602 Da the reaction can further proceed either (i) By reactions forming amides as the NH_2 usable for reaction with DMC do not lead to urethanes, or (ii) By further reaction of the residual NH groups in the urethane linkages with DMC-aminoacid. In effect, there is a peak at 610 Da (with Na^+) assigned to a compound formed in this latter manner by reaction of a third leucine of structure (IV)

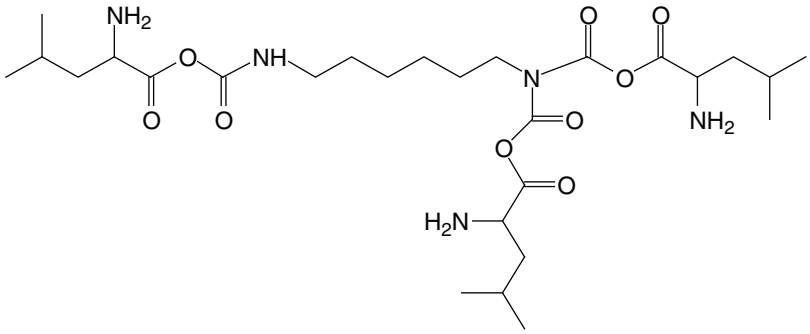

IV

And even the peak at 746 Da (without Na^+) of assigned structure (V):

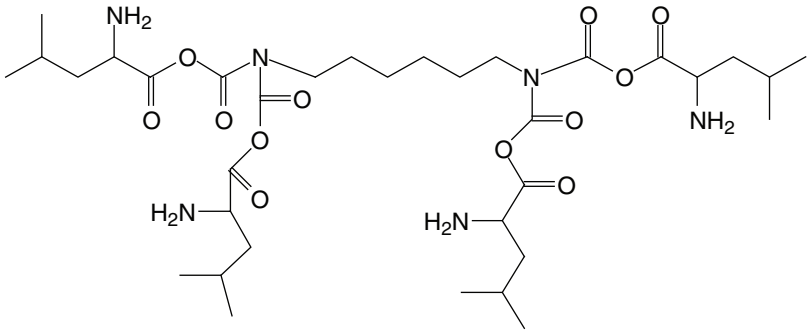

V

Similar peaks for other soy protein amino acids are also present.

There are then some urethane linkages formed, more than enough to cross-link the protein, even if these are coupled with lactam-like structures. Thus, once the two NH_2 of the diamine are saturated then any further reaction can proceed either (i) Through the formation of amides, hence polyamides [41], or (ii) By a chain reaction with any residual -NH- group that is obtained when forming a urethane linkage, or (iii) By using a polyamine rather than a diamine. This means that in any case the hardened network formed is most likely to be cross-linked by a mix of urethane bridges and amides ones.

Parasite side reactions also appear to occur as indicated by the peaks at 256 Da (VI) and 398 Da (VII) assigned to structures derived by the reaction of DMC with the diamine.

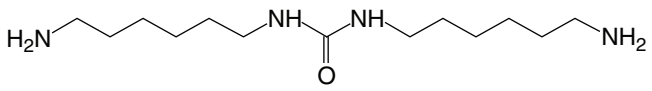

VI

And

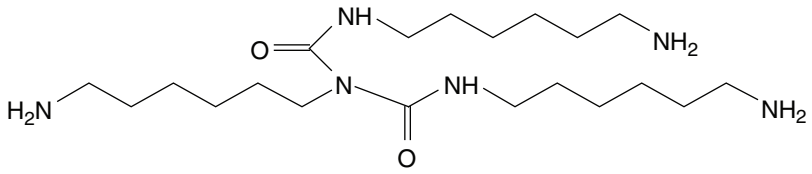

VII

Although these reactions form also compounds that are platforms for further urethane linkages to be formed either among themselves or with the SPI amino acids.

In summary rather complex tridimensional structures can results from these combinations.

The reaction of formation of soy protein urethanes, when using DMC as the carbonate, leads to urethanes that eventually share a lactam structure. The use of a longer carbonate, preferably cyclic such as propylene carbonate, does not eliminate the presence of such urethane/lactam type structures.

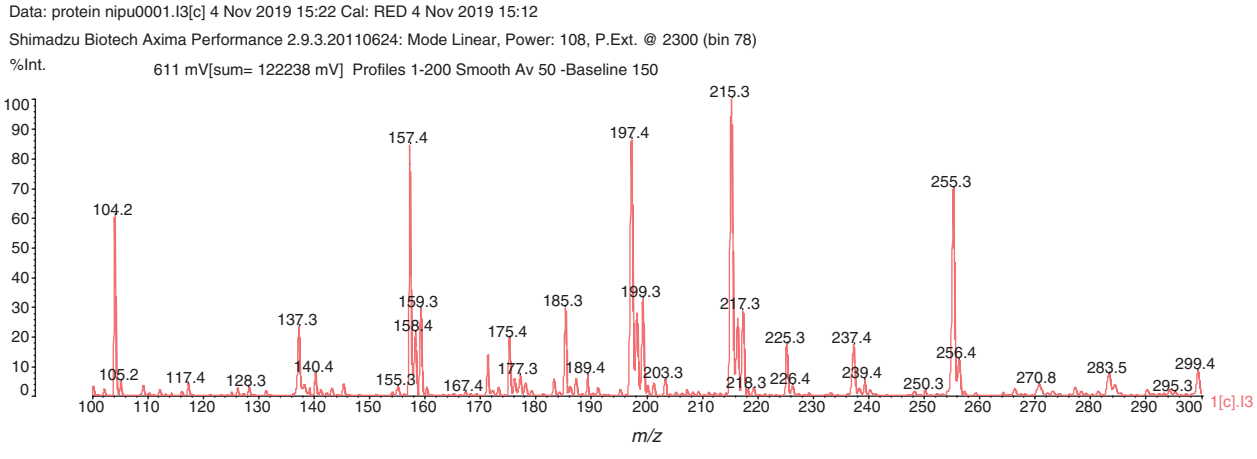

(a)

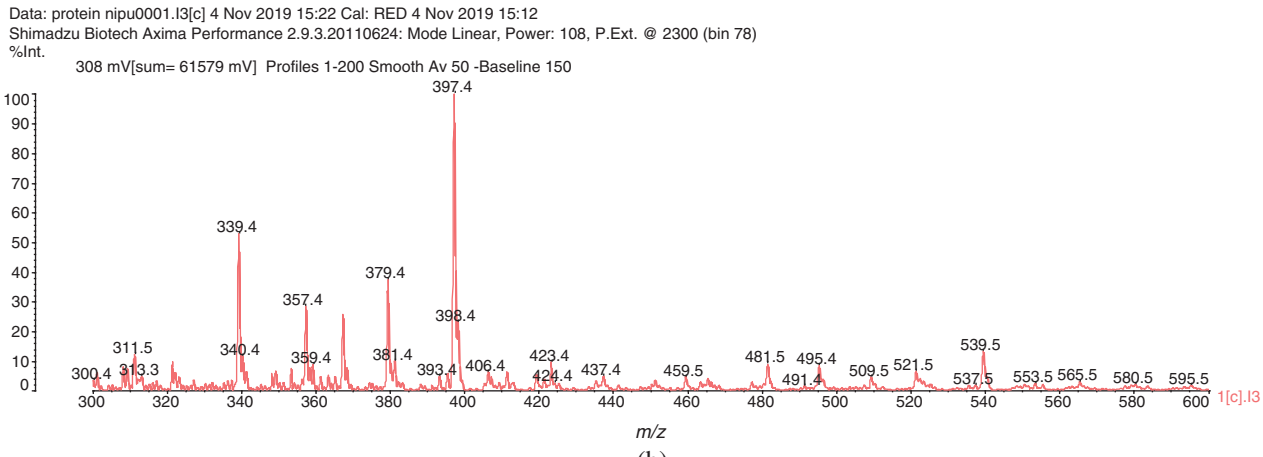

(b)

Figure 1: (continued)

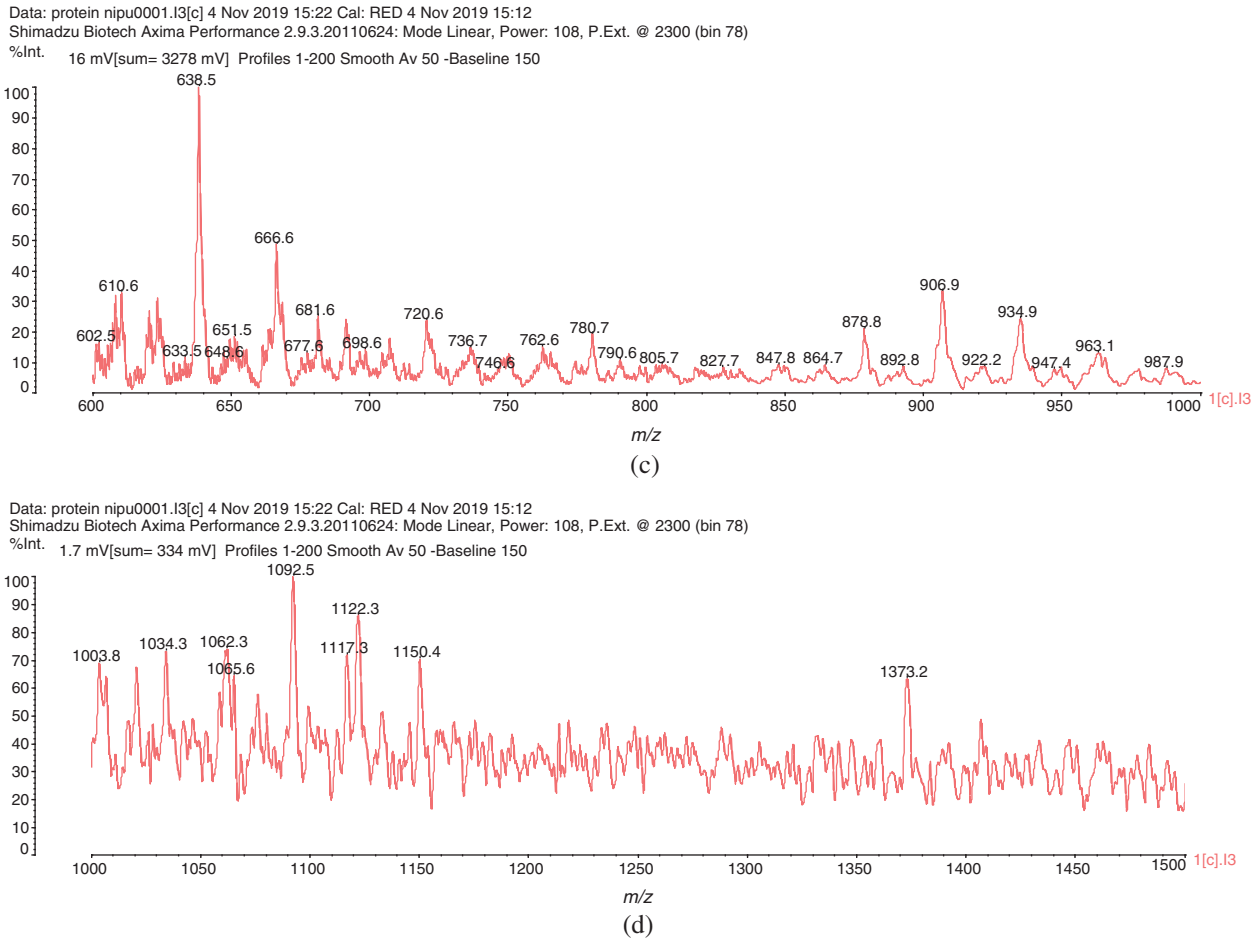

Figure 1: MALDI-ToF spectra of soy protein isolate-based non-isocyanate polyurethane (NIPU) adhesive. (a) 100–300 Da range. (b) 300–600 Da range. (c) 600–1000 Da range. (d) 1000–1500 Da range

The FTIR spectra of SPI and of the SPI-NIPU resin are shown in Fig. 2. The peaks at 1703 cm^{-1}, 1543 cm^{-1} and 1255 cm^{-1} are characteristic of the asymmetric stretching of urethane linkages, with the 1703 cm^{-1} for the SPI NIPU spectrum belonging the C=O of the urethane being quite intense and being absent in the spectrum of SPI alone. This conclusion of the presence of urethane linkages is confirmed by the presence of other peaks. Thus, the appearance of the relatively small peak at 1766 cm^{-1} in the SPI NIPU spectrum is characteristic the R-COO-R of esters derived from the lactam structures, these being esters of the carbamic acid (-NH-COO-) forming the urethanes, confirming the structures assigned by the MALDI-ToF analysis. The big peak at 1639 cm^{-1} is characteristic of amide groups, the peak being quite marked already for SPI alone, thus describing the amide (peptide) linkages holding together the protein skeleton. This same peak becomes even more dominant in the SPI NIPU spectrum where the amides derived from the reactions of the diamine with DMC and the proteins amino acids generate a great number of amides in the urethane structure superposed to the ones already present in the protein skeleton. The presence of the amide groups is supported by the peak at 1370 cm^{-1} (thus of-CO-NH-C-) and the wide peak at 3200 cm^{-1} that mask a number of different group effects. The peak at 1441 cm^{-1} represents the asymmetric stretch of -CH_2- groups of the alkane chains of the diamine included in the finished network. Lastly the peak at 1390–1400 cm^{-1} belongs to the protonated N-containing groups, such as -NH_3^+ on the protein aminoacids. The two sharp peaks at 2900 cm^{-1} and 2800 cm^{-1} are assigned to the asymmetric stretching of both the –CH_3 groups of DMC and the asymmetric stretching of the R-CH_2-R

chains from the amine, both before and after reaction. They support such assignments in relation to the peak at 1441 cm^{-1} for the $–CH_2$- groups. It must be also pointed out that these peaks are particularly intense as they are the superposition of the asymmetric stretching band of both $–CH_3$ and $–CH_2$- groups.

The thermomechanical analysis traces of SPI-NIPU adhesive is shown in Fig. 3. The curve of the increase of Young's modulus as a function of temperature show two upsurges and two peaks of MOE, namely at 130°C and at 220°C, this latter starting at around 185°C. The curves decrease in MOE value between the two peaks. This means that the peak at 130°C indicates the formation of an unstable network that is degraded and transformed if the temperature is increased causing a marked internal rearrangement. The second peak at higher temperature indicates that curing of the SPI-NIPU resin occurs at a high temperature as already reported in previous literature for similar types of adhesives [34,35]. The increase of Young's modulus has been shown to correlate with the bonding strength of the adhesive [42–48].

It is interesting to speculate what is the cause of the marked decrease between the two MOE peaks in Fig. 3. While it could be an unstable structure, a more likely reason could derive from the formation of linear polymers arranging themselves in a physically entangled network, rather than a chemically cross-linked one. As the temperature increases further, the Brownian movements would make the viscosity of these physically entangled chains markedly decrease and extensively disentangle, the MOE again starting to increase at the much higher temperature of the second peak once chemical cross-linking does finally occur.

Before the TMA curves show a significant increase in the modulus value, the overall trend of the modulus values in the TMA curves of the NIPU adhesive decreases between 50°C and 75°C. This is mainly due to the decrease in viscosity of the adhesive as the temperature increases, resulting in a lower viscosity and bonding strength. Conversely, the adhesive penetrates into the wood, softening or degrading it during heating thus reducing its strength. It is evident from the TMA trace that the curing temperature to be used for such adhesives is relatively higher than what common to-day for equivalent panels bonded with traditional adhesives. After 200°C degradation of the wood substrate is known to start [45–48], thus the second peak is rather high when considering that wood degradation has already started to occur at the same time. The decrease of the curve afterward is the reflexion of the continuing degradation of the wood substrate.

The results of the 3-plys plywood panels prepared are presented in Tab. 2. These indicate that the SPI NPU adhesive by itself just passes at 0.74 MPa the interior grade limit of the relevant China national standards [38–40] that requires a shear strength equal to, or higher than 0.7 MPa. By adding 10% and 15% biosourced GDE the dry shear strength results improved markedly in both cases passing to 1.34 MPa and 1.73 MPa respectively. This indicates that also the dry strength requirements for interior grade plywood of European Norm EN 636:2012 (2012) are satisfied [40] for interior grade plywood. Such a marked shear strength increase indicates that even the addition of smaller percentages of GDE, around 5% by weight, would be sufficient to comfortably pass the requirements for interior grade plywood panels under industrial conditions. The addition of GDE improves the performance due to additional cross-linking. The 24 hours cold water soaking results and the 3 hours at 63°C tests did not pass the requirements for exterior or semiexterior grade plywood as shown in Tab. 2 which are 0.7 MPa and 1.0 MPa for both the China National Standard and in the European Norm, respectively. This is consistent with the results of the TMA reported in Fig. 3, where it is indicated that these adhesives, in the reaction proportions used in this work, need a higher curing temperature to develop all their strength and achieve good results in the wet-type tests. It means also that such an adhesive under the conditions used is possibly better suited to its use in particleboard where higher pressing temperatures are used. An approach to explore to further decrease the high energy of activation of the curing reaction and thus achieve better wet bonding results would be to use small percentages of ionic liquids as already experienced for other adhesives [49].

Table 1: Assignment of structures to relevant MALDI-ToF peaks from Figs. 1a–1d

189 Da = reaction product of leucine with DMC, without Na^+

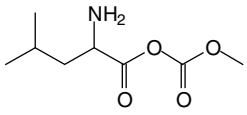

215 Da = 189 Da + Na^+

256 Da = Calculated 258 Da, no Na^+

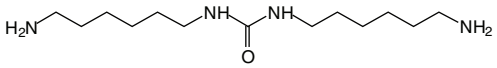

270 Da = triptofan-DMC

OR

270 = serine-DMC-Amine +Na^+

295 Da = leucine-DMC-Hexamethylene diamine + Na^+

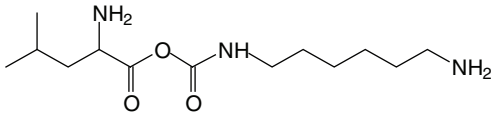

339 Da = the same as 295 Da but with arginine, thus arginine-DMC-amine + Na^+

368 Da = same as 295 Da but with tryptophan, thus Tryptophan-DMC-Amine + Na^+

398 Da =Calculated 400 Da, no Na^+; 423 Da with Na^+

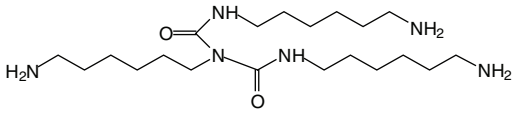

453 Da = The small peak at 453 Da is leucine-DMC-amine-DMC-leucine +Na^+

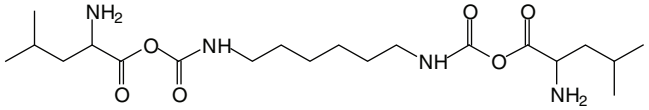

495 Da = leucine-DMC-amine-DMC-arginine + Na^+

539 Da = arginine-DMC-amine-DMC-arginine + Na^+

602 Da = tryptophan-DMC-amine-DMC-Tryptophan +Na^+

610 Da with Na^+

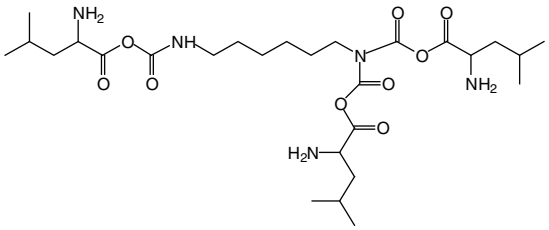

746 Da, no Na^+

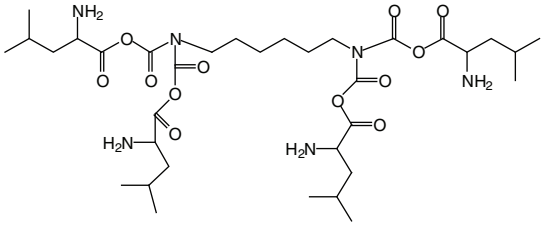

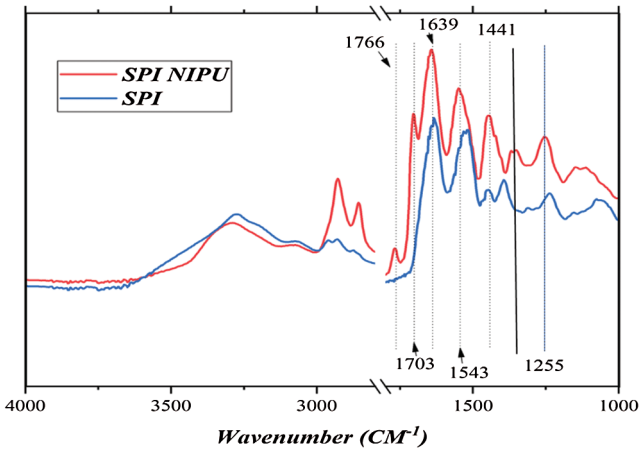

Figure 2: FT-IR spectra of soy protein isolate (SPI) and of soy protein isolate non-isocyanate polyurethane (NIPU) adhesive resin

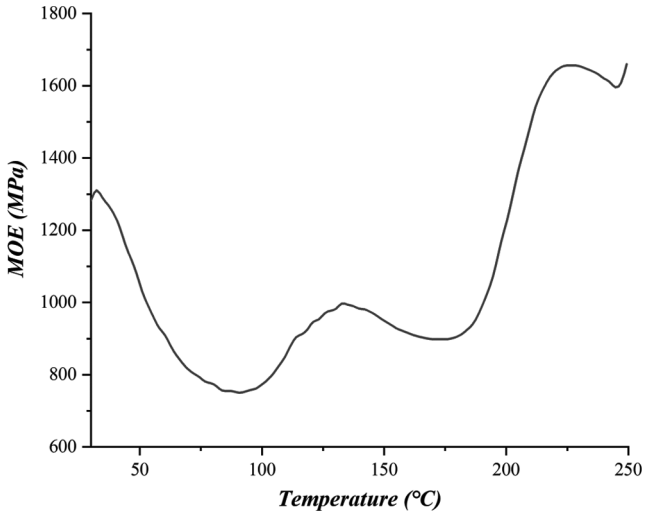

Figure 3: Thermomechanical analysis (TMA) curves of MOE as a function of temperature of joints bonded with soy protein isolate non-isocyanate polyurethane (NIPU) adhesive

Table 2: SPI-NIPU-bonded plywood test results. Percentages wood failure for the dry test are in parenthesis

		Shear Strength (MPa)	
	Dry	63°C for 3h	24 h cold water
SPI-NIPU	0.74	–	–
SPI-NIPU + 10%GDE	1.30 (30)	–	–
SPI-NIPU + 15%GDE	1.73 (90)	0.28	0.34

Note: (-) not tested.

4 Conclusions

Soy-protein isolate (SPI) has been used to prepare non-isocyanate polyurethane (NIPU) thermosetting adhesives for wood panels by reacting it with dimethyl carbonate (DMC) and hexamethylene diamine. MALDI-ToF and FTIR spectrometry have shown that urethane linkages are effectively formed in the reaction, in which all three reagents do participate. Some parasite reactions do occur, but these do not appear to detract to the formation of NIPU resins. Both linear as well as branched oligomers were obtained and identified, indicating by their molecular weight growth how such oligomer structures could further cross-link to form a hardened network. While the NIPU oligomers structures identified present the characteristics of urethane linkages derived from the urethane precursor carbamic acid (-NHCOOH-), they also simultaneously present structures characteristic of lactams. This is rather unusual, as they are exclusively due to the use of DMC, the simple organic carbonate used, and will not occur with other types of organic carbonates. Thermomechanical analysis (TMA) monitoring of the curing of the adhesive showed two distinct MOE maxima peaks, one around 130°C and the other around 220°C, with a very marked decrease in MOE between the two. The first peak can be assigned to the growth of linear oligomers forming a physically entangled network. This physically entangled network collapses and disentangles as the temperature increases due to the ever more marked Brownian movements of the linear oligomer chains. The second peak is assigned to the chemical cross-linking of the chains forming a hardened network. Plywood panels were prepared by bonding them with the SPI-NIPU wood adhesive and gave acceptable results for dry strength, with wet strength improving only after addition of 15% of a biosourced glycerol diglycidyl ether.

Funding Statement: The author(s) received no specific funding for this study.

Conflicts of Interest: The authors declare that there are no conflicts of interest regarding the publication of this paper.

References

1. Vnučec, D., Kutnar, A., Goršek, A. (2017). Soy-based adhesives for wood-bonding–A review. *Journal of Adhesion Science and Technology, 31(8),* 910–931. DOI 10.1080/01694243.2016.1237278.
2. Pizzi, A. (2016). Wood products and green chemistry. *Annals of Forest Science, 73(1),* 185–203. DOI 10.1007/s13595-014-0448-3.
3. Zhong, Z., Sun, X. S., Wang, D., Ratto, J. A. (2003). Wet strength and water resistance of modified soy protein adhesives and effects of drying treatment. *Journal of Polymers and the Environment, 11(4),* 137–144. DOI 10.1023/A:1026048213787.
4. Liu, Y., Li, K. (2002). Chemical modification of soy protein for wood adhesives. *Macromolecular Rapid Communications, 23,* 739–742.
5. Sun, X., Bian, K. (1999). Shear strength and water resistance of modified soy protein adhesives. *Journal of the American Oil Chemists' Society, 76(8),* 977–980. DOI 10.1007/s11746-999-0115-2.
6. Hettiarachchy, N. S., Kalapathy, U., Myers, D. J. (1995). Alkali-modified soy protein with improved adhesive and hydrophobic properties. *Journal of the American Oil Chemists' Society, 72(12),* 1461–1464. DOI 10.1007/BF02577838.
7. Lei, H., Du, G., Wu, Z., Xi, X., Dong, Z. (2014). Cross-linked soy-based wood adhesives for plywood. *International Journal of Adhesion and Adhesives, 50,* 199–203. DOI 10.1016/j.ijadhadh.2014.01.026.
8. Eslah, F., Jonoobi, M., Faezipour, M., Asharpour, M., Enayati, A. A. (2016). Preparation and development of a chemically modified bio-adhesive derived from soybean flour protein. *International Journal of Adhesion and Adhesives, 71,* 48–54. DOI 10.1016/j.ijadhadh.2016.08.011.
9. Lin, Q., Chen, N., Bian, L., Fan, M. (2012). Development and mechanism characterization of high performance soy-based bio-adhesives. *International Journal of Adhesion and Adhesives, 34,* 11–16. DOI 10.1016/j.ijadhadh.2012.01.005.

10. Ghahri, S., Pizzi, A., Mohebby, B., Mirshoktaie, A., Mansouri, H. R. et al. (2018). Improving water resistance of soy-based adhesive by vegetable tannin. *Journal of Polymers and the Environment, 26(5),* 1881–1890. DOI 10.1007/s10924-017-1090-6.
11. Ghahri, S., Pizzi, A., Mohebby, B., Mirshoktaie, A., Mansouri, H. R. et al. (2018). Soy-based, tannin-modified plywood adhesives. *Journal of Adhesion, 94(3),* 218–237. DOI 10.1080/00218464.2016.1258310.
12. Ghahri, S., Pizzi, A. (2018). Improving soy-based adhesives for wood particleboard by tannins addition. *Wood Science and Technology, 52(1),* 261–279. DOI 10.1007/s00226-017-0957-y.
13. Frihart, C. R., Lorenz, L. (2019). Specific oxidants improve the wood bonding strength of soy and other plant flours. *Journal of Polymer Science Part A: Polymer Chemistry, 57(9),* 1017–1023. DOI 10.1002/pola.29357.
14. Frihart, C. R., Pizzi, A., Xi, X., Lorenz, L. (2019). Reactions of soy flour and soy protein by non-volatile aldehydes generation by specific oxidation. *Polymers, 11(9),* 1478. DOI 10.3390/polym11091478.
15. Lei, H., Pizzi, A., Navarrete, P., Rigolet, S., Redl, A. et al. (2010). Gluten protein adhesives for wood panels. *Journal of Adhesion Science and Technology, 24(8–10),* 1583–1596. DOI 10.1163/016942410X500963.
16. Wescott, J. M., Traska, A., Frihart, C. R. (2005). Durable soy-based adhesive dispersions. Wood adhesives. San Diego, California, USA. Forest Products Society, Madison, WI, 2005, 263–269.
17. Kathalewar, M. S., Joshi, P. B., Sabnis, A. S., Malshe, V. C. (2013). Non-isocyanate polyurethanes: From chemistry to applications. *RSC Advances, 3(13),* 4110–4129. DOI 10.1039/c2ra21938g.
18. Poussard, L., Mariage, J., Grignard, B., Detrembleur, C., Jérôme, C. et al. (2016). Non-isocyanate polyurethanes from carbonated soybean oil using monomeric or oligomeric diamines to achieve thermosets or thermoplastics. *Macromolecules, 49(6),* 2162–2171. DOI 10.1021/acs.macromol.5b02467.
19. Ochiai, B., Utsuno, T. (2013). Non-isocyanate synthesis and application of telechelic polyurethanes via polycondensation of diurethanes obtained from ethylene carbonate and diamines. *Journal of Polymer Science Part A: Polymer Chemistry, 51(3),* 525–533. DOI 10.1002/pola.26418.
20. Figovsky, O., Shapovalov, L., Leykin, A., Birukova, O., Potashnikova, R. (2013). Recent advances in the development of non-isocyanate polyurethanes based on cyclic carbonates. *PU Magazine, 10,* 1–9.
21. Rokicki, G., Parzuchowski, P. G., Mazurek, M. (2015). Non-isocyanate polyurethanes: Synthesis, properties, and applications. *Polymers for Advanced Technologies, 26(7),* 707–761. DOI 10.1002/pat.3522.
22. Noreen, A., Zia, K. M., Zuber, M., Ameer, S. T., Zahoor, F. (2016). Bio-based polyurethane: An efficient and environment friendly coating systems: A review. *Progress in Organic Coatings, 91,* 25–32. DOI 10.1016/j.porgcoat.2015.11.018.
23. Birukov, O., Potashnikova, R., Leykin, A., Figovsky, O., Shapovalov, L. (2009). Advantages in chemistry and technology of non-isocyanate polyurethane. *Journal of the Scientific Israel-Technological Advances, 11,* 160–167.
24. Kathalewar, M., Sabnis, A., Waghoo, G. (2013). Effect of incorporation of surface treated zinc oxide on non-isocyanate polyurethane based nano-composite coatings. *Progress in Organic Coatings, 76(9),* 1215–1229. DOI 10.1016/j.porgcoat.2013.03.027.
25. Grignard, B., Thomassin, J. M., Gennen, S., Poussard, L., Bonnaud, L. et al. (2016). CO_2-blown microcellular non-isocyanate polyurethane (NIPU) foams: From bio-and CO_2-sourced monomers to potentially thermal insulating materials. *Green Chemistry, 18(7),* 2206–2215. DOI 10.1039/C5GC02723C.
26. Cornille, A., Guillet, C., Benyahya, S., Negrell, C., Boutevin, B. et al. (2016). Room temperature flexible isocyanate-free polyurethane foams. *European Polymer Journal, 84,* 873–888. DOI 10.1016/j.eurpolymj.2016.05.032.
27. Thébault, M., Pizzi, A., Dumarçay, S., Gerardin, P., Fredon, E. et al. (2014). Polyurethanes from hydrolysable tannins obtained without using isocyanates. *Industrial Crops and Products, 59,* 329–336. DOI 10.1016/j.indcrop.2014.05.036.
28. Thébault, M., Pizzi, A., Essawy, H. A., Barhoum, A., Van Assche, G. (2015). Isocyanate free condensed tannin-based polyurethanes. *European Polymer Journal, 67,* 513–526. DOI 10.1016/j.eurpolymj.2014.10.022.
29. Thébault, M., Pizzi, A., Santiago-Medina, F. J., Al-Marzouki, F. M., Abdalla, S. (2017). Isocyanate-free polyurethanes by coreaction of condensed tannins with aminated tannins. *Journal of Renewable Materials, 5 (1),* 21–29.

30. Xi, X., Pizzi, A., Gerardin, C., Du, G. (2018). Glucose-biobased non-isocyanate polyurethane rigid foams. *Journal of Renewable Materials, 7(3),* 301–312. DOI 10.32604/jrm.2019.04174.
31. Xi, X., Pizzi, A., Gerardin, C., Lei, H., Chen, X. et al. (2019). Preparation and evaluation of glucose based non-isocyanate polyurethane self-blowing rigid foams. *Polymers, 11(11),* 1802. DOI 10.3390/polym11111802.
32. Chen, X., Li, J., Xi, X., Pizzi, A. Zhou, X. et al. (2020). Condensed tannin-glucose-based NIPU bio-foams of improved fire retardancy. *Polymer Degradation and Stability, 175,* 109121. DOI 10.1016/j.polymdegradstab.2020.109121.
33. Chen, X., Xi, X., Pizzi, A., Fredon, E., Zhou, X. et al. (2020). Preparation and characterization of condensed tannin non-isocyanate polyurethane (NIPU) rigid foams by ambient temperature blowing. *Polymers, 12(4),* 750. DOI 10.3390/polym12040750.
34. Xi, X., Pizzi, A., Delmotte, L. (2018). Isocyanate-free polyurethane coatings and adhesives from mono-and di-saccharides. *Polymers, 10(4),* 402. DOI 10.3390/polym10040402.
35. Xi, X., Wu, Z., Pizzi, A., Gerardin, C., Lei, H. et al. (2019). Non-isocyanate polyurethane adhesive from sucrose used for particleboard. *Wood Science and Technology, 53(2),* 393–405. DOI 10.1007/s00226-019-01083-2.
36. Santiago-Medina, F. J., Basso, M. C., Pizzi, A., Delmotte, L. (2018). Polyurethanes from Kraft lignin without using isocyanates. *Journal of Renewable Materials, 6(4),* 413–425. DOI 10.7569/JRM.2017.634172.
37. Pizzi, A. (2019). Tannin-based Biofoams. *Journal of Renewable Materials, 7(5),* 477–492. DOI 10.32604/jrm.2019.06511.
38. China National Standard GB/T 14074 (2006). Testing methods for wood adhesives and their resins.
39. China National Standard GB/T17657-2013 (2013). Test methods for evaluating the properties of wood-based panels and surface decorated wood-based panels.
40. European Norm EN 636: 2012 (2012). Plywood–Specifications, Standardization Committee, European Commission, Bruxelles, Belgium.
41. Xi, X., Pizzi, A., Gerardin, C., Chen, X., Amirou, S. (2020). Soy protein isolate based polyamides as wood adhesives. *Wood Science and Technology, 54(1),* 89–102. DOI 10.1007/s00226-019-01141-9.
42. Pizzi, A., Garcia, R., Deglise, X. (1998). Thermomechanical analysis of entanglement networks - correlation of some calculated and experimental parameters. *Journal of Applied Polymer Science, 67,* 1673–1678.
43. Kamoun, C., Pizzi, A. (2000). Particleboard I.B. forecast by TMA bending in MUF adhesives curing. *Holz als Roh- und Werkstoff, 58, 4(4),* 288–289. DOI 10.1007/s001070050428.
44. Lecourt, M., Humphrey, P., Pizzi, A. (2003). Comparison of TMA and ABES as forecasting systems of wood bonding effectiveness. *Holz als Roh- und Werkstoff, 61(1),* 75–76. DOI 10.1007/s00107-002-0346-5.
45. Pizzi, A., Garcia, R., Deglise, X. (1998). Thermomechanical analysis of entanglement networks–correlation of some calculated and experimental parameters. *Journal of Applied Polymer Science, 67,* 1673–1678.
46. Garcia, R., Pizzi, A. (1998). Cross-linked and entanglement networks in thermomechanical analysis of polycondensation resins. *Journal of Applied Polymer Science, 70,* 1111–1116.
47. Kamoun, C., Pizzi, A., Garcia, R. (1998). The effect of humidity on crosslinked and entanglement networking of formaldehyde-based wood adhesives. *Holz als Roh- und Werkstoff, 56(4),* 235–243. DOI 10.1007/s001070050309.
48. Pizzi, A., Lu, X., Garcia, R. (1999). Lignocellulosic substrates influence on TTT and CHT curing diagrams of polycondensation resins. *Journal of Applied Polymer Science, 71,* 915–925.
49. Younesi-Kordkheili, H., Pizzi, A. (2016). Acid ionic liquids as a new hardener in urea-glyoxal adhesive resins. *Polymers, 8(3),* 57–71. DOI 10.3390/polym8030057.